Proc. Natl. Acad. Sci. USA
Vol. 96, pp. 10812–10817, September 1999
Medical Sciences

Targeted gene disruption reveals an essential role for ceruloplasmin in cellular iron efflux

Z. Leah Harris, Alison P. Durley, Tsz Kwong Man, and Jonathan D. Gitlin*

Edward Mallinckrodt Department of Pediatrics, Washington University School of Medicine, St. Louis, MO 63110

Edited by William S. Sly, Saint Louis University School of Medicine, St. Louis, MO, and approved July 20, 1999 (received for review May 11, 1999)

ABSTRACT **Aceruloplasminemia is an autosomal recessive disorder of iron metabolism. Affected individuals evidence iron accumulation in tissue parenchyma in association with absent serum ceruloplasmin. Genetic studies of such patients reveal inherited mutations in the ceruloplasmin gene. To elucidate the role of ceruloplasmin in iron homeostasis, we created an animal model of aceruloplasminemia by disrupting the murine ceruloplasmin (*Cp*) gene. Although normal at birth, $Cp^{-/-}$ mice demonstrate progressive accumulation of iron such that by one year of age all animals have a prominent elevation in serum ferritin and a 3- to 6-fold increase in the iron content of the liver and spleen. Histological analysis of affected tissues in these mice shows abundant iron stores within reticuloendothelial cells and hepatocytes. Ferrokinetic studies in $Cp^{+/+}$ and $Cp^{-/-}$ mice reveal equivalent rates of iron absorption and plasma iron turnover, suggesting that iron accumulation results from altered compartmentalization within the iron cycle. Consistent with this concept, $Cp^{-/-}$ mice showed no abnormalities in cellular iron uptake but a striking impairment in the movement of iron out of reticuloendothelial cells and hepatocytes. Our findings reveal an essential physiologic role for ceruloplasmin in determining the rate of iron efflux from cells with mobilizable iron stores.**

The metabolism of iron is characterized by a remarkably efficient process of recycling. This is accomplished by a daily sequence of internal iron exchange such that nearly 30 times the amount of iron acquired or lost each day is transported through the red cell cycle (1). Homeostasis is achieved as the amount of iron equivalent to that utilized for erythropoiesis is returned to the plasma from the reticuloendothelial cell compartment after the catabolism of senescent erythrocytes. Although this outflow of iron from reticuloendothelial cells in the liver and spleen represents the single largest efflux of iron from cells in the body, the mechanisms underlying this process remain entirely unknown (2). The importance of elucidating these mechanisms is highlighted clinically by the iron overload disorders, which represent a substantial component of hematologic disease for which increased understanding and novel therapeutic approaches are needed (3, 4).

Aceruloplasminemia is an autosomal recessive disorder of iron metabolism (5). Affected individuals sustain an insidious, long-term accumulation of parenchymal iron equivalent to that observed in hereditary hemochromatosis that results in diabetes, retinal degeneration, and neurologic symptoms (6–8). In all cases, there is a complete absence of serum ceruloplasmin, and molecular genetic analysis has revealed specific inherited mutations in the ceruloplasmin gene (9, 10). Despite some similarities with other iron-overload syndromes, aceruloplasminemia is unique in that the neurologic manifestations dominate the clinical picture. All patients eventually succumb from the effects of increased iron accumulation within the basal ganglia. Taken together with recent work indicating an essential role for a homologous copper protein in gastrointestinal iron absorption (11), these clinical observations reveal a critical function for multicopper oxidases in human iron metabolism.

Despite the careful clinical description of aceruloplasminemia, the role of ceruloplasmin in iron homeostasis has not been elucidated. Early studies in copper-deficient animals revealed impaired reticuloendothelial cell iron release that was corrected by the administration of ceruloplasmin, implying a role for this protein as a plasma ferroxidase regulating tissue iron efflux (12–14). However, such studies were clouded by the effects of copper deficiency in these animals, and more recent work with cultured cell lines *in vitro* has suggested a role for ceruloplasmin in cellular iron influx (15, 16). Understanding how ceruloplasmin affects iron homeostasis is essential for the development of effective therapies in aceruloplasminemia and may provide new insight into the pathogenesis of iron overload. We therefore initiated this current study to develop an animal model of aceruloplasminemia in which these mechanisms of iron homeostasis could be experimentally addressed.

MATERIALS AND METHODS

Generation of Aceruloplasminemic Mice. A cDNA clone corresponding to the carboxyl terminus of murine ceruloplasmin was used to screen a murine 129/SvJ genomic library in λ phage (17). Nucleotide sequence analysis identified three overlapping clones encompassing the last eight exons of the murine ceruloplasmin gene. The genomic region corresponding to exons 14 through part of exon 17 was amplified by PCR and subcloned into the unique *Xho*I site in the pPNT targeting vector upstream of the *Neo* gene (18). Similarly, a region corresponding to the terminal portion of exon 18 through 19 was amplified and subcloned into the unique *Kpn*I site. This targeting strategy replaced almost all of exons 17 and 18 of the murine ceruloplasmin gene with the PGK*neo* cassette. Targeting vector (25 μg) was linearized with *Not*I and introduced into the 129/Sv embryonic stem cell line RW4 (Genome Systems, St. Louis) by electroporation. After 36 hr, cells were selected in the presence of 500 μg/ml G418 (GIBCO/BRL) and 2 μM ganciclovir (Syntex, Palo Alto, CA) for 7 days. Genomic DNA from resistant clones was digested with *Bgl*II and hybridized with a cDNA clone encoding exons 12 and 13 of the murine ceruloplasmin gene. Two independent clones were injected into blastocysts of C57BL/6J mice and transferred into pseudopregnant female mice (19). Chimeric offspring were bred to black Swiss–Webster females, and tail DNA from the agouti offspring was analyzed to confirm transmission of the targeted allele. Heterozygous matings of F_1 mice produced homozygous animals. The genetic identity of these offspring was confirmed by amplification of tail DNA by

The publication costs of this article were defrayed in part by page charge payment. This article must therefore be hereby marked "*advertisement*" in accordance with 18 U.S.C. §1734 solely to indicate this fact.

PNAS is available online at www.pnas.org.

This paper was submitted directly (Track II) to the *Proceedings* office.

*To whom reprint requests should be addressed at: St. Louis Children's Hospital, One Children's Place, St. Louis, MO 63110. E-mail: gitlin@kids.wustl.edu.

PCR using oligonucleotide primers corresponding to exon 16 and either the end of exon 17 or the *Neo* gene.

Immunoblotting and Oxidase Assay. Serum was isolated from whole blood obtained by retroorbital phlebotomy. A 20-μl sample of serum from each mouse was separated by SDS/PAGE under reducing conditions, transferred to nitrocellulose membranes, and analyzed after incubation with rabbit polyclonal anti-human ceruloplasmin antisera as described previously (17). Ferroxidase activity was assayed in 5 μl of fresh serum after incubation with a solution containing 55 μM apotransferrin, 100 μM ascorbate, 60 μM $Fe(NH_4)_2(SO_4)_2$ in 0.0133 M phosphate buffer, pH 7.35. Activity was quantified by measuring the A_{460} at 5 and 15 min, using human ceruloplasmin as a positive control (20).

Iron Measurements, Hematological Parameters, and Histology. Retroorbital phlebotomy was used to obtain 200 μl of serum for determination of serum iron and total iron binding capacity (TIBC) with a kit from Sigma. Transferrin saturation was calculated as serum iron ÷ TIBC. Serum ferritin was determined on these same samples by using a Cobas Fara II chemical analyzer (Genox, Baltimore). For iron content, tissues were dried, weighed, and digested in 3 M HCl/10% trichloroacetic acid at 65°C for 20 hr. Then 20 μl of acid extract was incubated with bathophenanthroline chromogen and iron was quantitated as A_{535} (21). Hemoglobin, hematocrit, and mean red cell corpuscular volume were determined by Coulter automated analysis. For histology, tissues were fixed in 10% formalin, embedded in paraffin, sectioned, and mounted on slides for staining with hematoxylin and eosin or Perls' Prussian blue stain to detect storage iron.

Iron Absorption, Turnover, and Distribution. $^{59}FeCl_3$ was purchased from New England Nuclear (specific activity 32.4 mCi/mg; 1 mCi = 37 MBq). To measure iron absorption, mice were fasted overnight and gavaged with 0.1 ml of ^{59}Fe (500 μCi, 15 μg of iron) in 1.0 M ascorbic acid in PBS. Mice were exsanguinated at specific time points, and ^{59}Fe in organs, blood, and carcass was determined by using a Packard Cobra II γ counter. The percent iron absorbed at 72 hr was determined from the amount of ^{59}Fe in the entire animal, excluding the gastrointestinal tract (22). Iron clearance was determined in plasma samples obtained at 10- to 30-min intervals from 10 min to 6 hr after the i.v. injection of 2 μCi of ^{59}Fe in 50 μl of 0.1 M citric acid, pH 6.6. In some experiments mice were injected 10 min previously with 70 μg of iron in 0.1 ml of ferric citrate in 0.1 M citric acid, pH 6.6, to saturate plasma transferrin prior to ^{59}Fe clearance and distribution studies (22). The plasma iron turnover (PIT) was calculated as the plasma iron concentration divided by the plasma iron disappearance rate ($t_{1/2}$). To determine the ^{59}Fe tissue distribution, animals were sacrificed at various times after injection and perfused with PBS via cardiac puncture to remove blood from organs, and radioactivity was measured in weighed tissue samples (22).

Experimental Red Blood Cell Protocols. Whole blood was obtained in a heparinized syringe from wild-type mice by cardiac puncture. Red cells were obtained after centrifugation at 8,000 × *g* for 5 min, damaged by heating in PBS, pH 7.4, at 52°C for 30 min, and washed extensively in PBS, pH 7.4. $Cp^{+/+}$ and $Cp^{-/-}$ mice were injected via tail vein with a volume of heat-damaged red blood cells to deliver 2 μg of iron per g of mouse (23). Serum iron was determined as described above. Apoceruloplasmin was prepared from purified human serum ceruloplasmin by heating at 100°C for 7 min, followed by ferroxidase assay to confirm the loss of enzymatic activity. Mice were made anemic by retroorbital bleeding to remove 15% of their total circulating blood volume daily. A 20-μl sample of whole blood was used to measure hemoglobin as described above.

Animal Husbandry and Data Analysis. Mice were housed on a 12:12 light/dark cycle with ad libitum access to rodent chow (Purina, 0.02% wt/wt iron). $Cp^{-/-}$ mice were maintained on an outbred genetic background with wild-type littermates used as controls. Newborn pups were genotyped at 3 weeks of age as described above. For all experiments, including histologic studies, a minimum of three animals in each group were analyzed. Statistical analysis was by unpaired *t* test with significance defined as $P < 0.001$. All mouse protocols were in accordance with the National Institutes of Health guidelines and approved by the Animal Care and Use Committee of Washington University School of Medicine.

RESULTS

Targeted Deletion of Murine *Cp*. To generate a murine model of aceruloplasminemia a gene-targeting strategy was developed that eliminated exons 17 and 18 encoding residues essential for formation of the trinuclear copper cluster of ceruloplasmin (Fig. 1*A*). Southern analysis confirmed homologous recombination in embryonic stem cells (data not shown), and PCR amplification using the oligonucleotides indicated in Fig. 1*A* revealed the successful production of homozygous null mice (Fig. 1*B*). Immunoblot analysis of serum from $Cp^{+/+}$, $Cp^{+/-}$, and $Cp^{-/-}$ mice revealed a 50% reduction in ceruloplasmin in $Cp^{+/-}$ mice and a complete absence of this protein in $Cp^{-/-}$ mice (Fig. 1*C*). As anticipated from these results, serum ferroxidase activity measured by the formation of Fe^{3+}-transferrin was reduced in $Cp^{+/-}$ mice and negligible in $Cp^{-/-}$ mice (Fig. 1*D*).

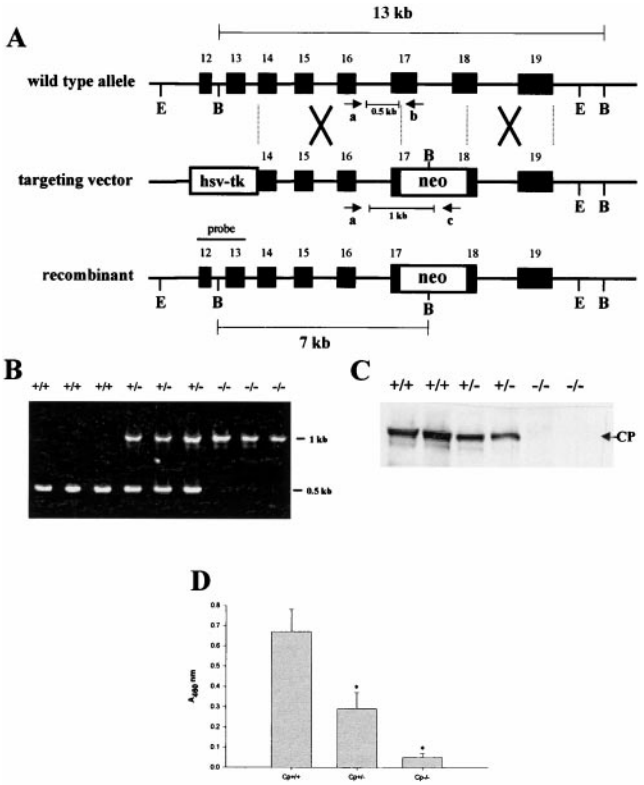

FIG. 1. Targeted disruption of the ceruloplasmin gene. (*A*) *Cp* locus, targeting vector and predicted recombinant allele. The 5′ flanking probe used for Southern analysis is shown. Restriction sites: E, *Eco*RV; B, *Bgl*II. (*B*) PCR products from tail genomic DNA corresponding to a 0.5-kb fragment (made by using primers a and b) from exon 16 to exon 17 in $Cp^{+/+}$ alleles and a 1.0-kb fragment (made by using primers c and d) from exon 16 to the Neo cassette in $Cp^{-/-}$ mice. (*C*) Immunoblot analysis of ceruloplasmin in serum from $Cp^{+/+}$, $Cp^{+/-}$, and $Cp^{-/-}$ mice. (*D*) Ferroxidase activity in serum of $Cp^{+/+}$, $Cp^{+/-}$, and $Cp^{-/-}$ mice. Results are expressed as means ± standard deviations; *, $P < 0.001$.

Table 1. Serum and tissue iron values in aceruloplasminemic mice

Mice	Hb, g/dl	Serum iron, μg/dl	TIBC, μg/dl	Transferrin saturation, %	Ferritin, ng/ml	Iron content, μg/g dry wt	
						Liver	Spleen
$Cp^{+/+}$	14.1 ± 3.3	252 ± 25	477 ± 45	43 ± 7	112 ± 10	252 ± 64	224 ± 63
$Cp^{-/-}$	13.9 ± 3.4	245 ± 100	517 ± 30	33 ± 5	410 ± 103*	666 ± 130*	1,294 ± 94*

Values are means ± standard deviations, $n = 3$ from each group at 1 year of age. Hb, hemoglobin; (Hb), TIBC, total iron binding capacity. Significant differences were observed between $Cp^{+/+}$ and $Cp^{-/-}$ mice for serum ferritin, (*, $P < 0.001$), liver tissue iron content, (*, $P < 0.001$), and spleen tissue iron content (*, $P < 0.001$ in all cases).

Iron-Overload Phenotype. $Cp^{-/-}$ mice were normal at birth and exhibited normal growth, fertility, and longevity. However, by 6 months of age $Cp^{-/-}$ mice fed ad libitum on a normal chow diet evidenced clear differences in the iron content of the liver and spleen, reaching levels of iron 3- to 6-fold greater than that seen in $Cp^{+/+}$ or $Cp^{+/-}$ littermates by 1 year of age (Table 1). While hematologic and serum iron values remained normal in $Cp^{-/-}$ mice at this age, the serum ferritin concentration was significantly increased compared with that of littermate controls, presumably reflecting the increase in hepatic and splenic iron stores (Table 1).

The difference in tissue iron content in $Cp^{+/+}$ and $Cp^{-/-}$ mice was readily apparent upon microscopic examination of affected tissues (Fig. 2). Although the liver architecture in $Cp^{-/-}$ mice was normal (Fig. 2*A*), Perls' staining revealed abundant storage iron throughout the liver parenchyma when compared with $Cp^{+/+}$ littermates (Fig. 2 *B* and *C*). This excess iron was found diffusely distributed throughout the cytoplasm of all hepatocytes and as somewhat larger inclusions within reticuloendothelial (Kupffer) cells (Fig. 2*D*). Examination of splenic tissue from $Cp^{-/-}$ mice revealed a similar finding, with a marked increase in storage iron content throughout the reticuloendothelial cells of this tissue (Fig. 2 *E* and *F*).

Reticuloendothelial Cell Iron Efflux. Ferrokinetic studies in $Cp^{-/-}$ mice (10–16 weeks old), using $Cp^{+/+}$ littermates as controls, failed to reveal any differences in the rate of iron absorption, initial tissue iron distribution, or plasma iron turnover under steady-state conditions (Table 2). These findings suggested that the increased tissue iron in $Cp^{-/-}$ mice might result from a slow but continuous accumulation of parenchymal iron secondary to impaired cellular efflux. To examine this hypothesis, serum iron concentrations were measured in $Cp^{+/+}$ and $Cp^{-/-}$ mice after the infusion of heat-damaged red blood cells. Under these circumstances, the excess iron derived from the infused red blood cells is rapidly released from the reticuloendothelial system into the plasma (23, 24). To eliminate the possibility that excess iron stores in $Cp^{-/-}$ mice might affect these results, mice were chosen for these experiments at an age before the onset of detectable differences in tissue iron stores. Serum iron concentrations measured 15 min after infusion confirmed the absence of hemolysis (data not shown). As anticipated, $Cp^{+/+}$ mice demonstrated a steady increase in serum iron after the infusion of

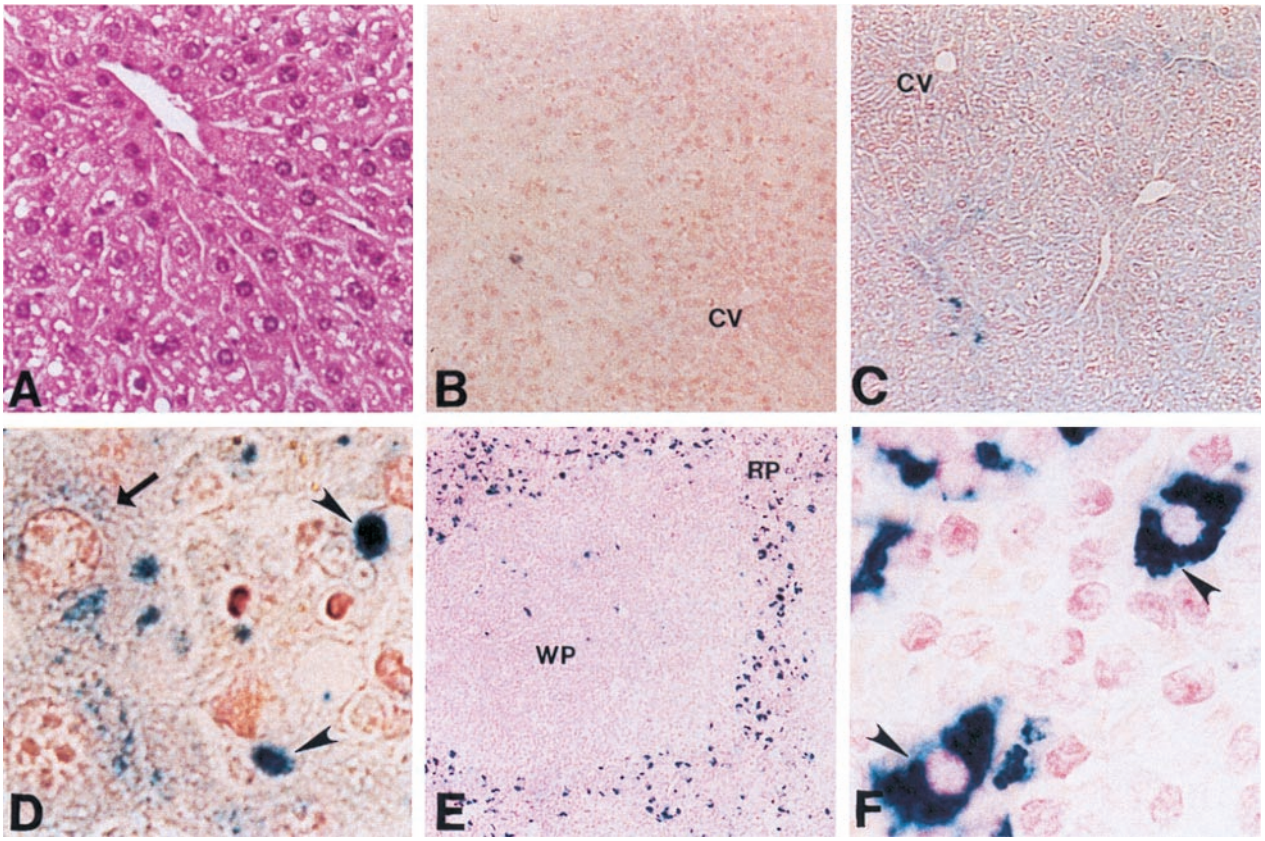

FIG. 2. (*A*) Hematoxylin/eosin stain of liver from a representative 1-year-old $Cp^{-/-}$ animal (×17). (*B*) Perls' stain of liver section from a representative 1-year-old $Cp^{+/+}$ mouse (×8.5). CV, central vein. (*C*) Perls' stain of liver section from $Cp^{-/-}$ littermate (×8.5). (*D*) High-power view from *C* (×100). Arrow indicates iron accumulation in hepatocyte; arrowheads indicate Kupffer cells. (*E*) Perls' stain of $Cp^{-/-}$ spleen from 1-year-old mouse (×8.5). RP, red pulp; WP, white pulp. (*F*) High-power view from *E* (×100). Arrowheads indicate iron within splenic reticuloendothelial cells.

Table 2. Iron absorption, distribution, and turnover in aceruloplasminemic mice

Mice	Iron absorption, % total ^{59}Fe dose absorbed	Iron distribution		Plasma iron turnover, μg/dl/min	
		Organ	% ^{59}Fe absorbed	Before phlebotomy	After phlebotomy
$Cp^{+/+}$	16 ± 6	Liver	9 ± 1	1.6–2.3	3.4–4.2
		Spleen	1 ± 0.1		
		RBC	50 ± 5		
$Cp^{-/-}$	12 ± 3	Liver	10 ± 2	2.2–2.6	1.6–2.2
		Spleen	1		
		RBC	52 ± 4		

Values are means ± standard deviations, $n = 6$ from each group. Plasma iron turnover was determined in $Cp^{+/+}$ and $Cp^{-/-}$ mice before and after 7 days of serial phlebotomy. A significant difference was observed in plasma iron turnover between $Cp^{+/+}$ and $Cp^{-/-}$ mice after phlebotomy (*, $P < 0.005$).

damaged red cells, reflecting the normal efflux of this metal from reticuloendothelial cells in the liver and spleen (Fig. 3*A*). However, in marked contrast to these observations, the serum iron concentration was unchanged throughout the entire time course of these experiments in $Cp^{-/-}$ mice administered an equivalent amount of iron as heat-damaged red blood cells (Fig. 3*A*). The changes in plasma iron content in $Cp^{+/+}$ mice were specific for the damaged red blood cells and not caused by changes secondary to the volume of blood withdrawn at each experimental time point, as serum iron concentrations were unchanged in $Cp^{+/+}$ mice not having received an infusion but bled at similar intervals (data not shown).

The studies of heat-damaged red cells suggested that ceruloplasmin may be essential for determining the rate of reticuloendothelial cell iron efflux under these conditions. To directly examine the effect of ceruloplasmin in mediating the iron efflux observed in $Cp^{+/+}$ mice, these experiments were repeated, and 3 hr after administration of heat-damaged red blood cells, purified human ceruloplasmin was injected i.v. to achieve a plasma level equivalent to approximately 20% of the normal murine ceruloplasmin concentration. Whereas no effect on serum iron concentration was observed in $Cp^{+/+}$ mice (data not shown), ceruloplasmin administration to $Cp^{-/-}$ mice resulted in a dramatic and rapid rise in the serum iron, which remained elevated for several hours after this infusion (Fig. 3*B*). This effect was specific for ceruloplasmin and not caused by changes in plasma volume associated with the infusion, as no change in the serum iron was observed in $Cp^{-/-}$ mice administered apoceruloplasmin (Fig. 3*B*), transferrin, or apotransferrin (data not shown).

The experiments with damaged red blood cells revealed an impairment in reticuloendothelial cell iron efflux in $Cp^{-/-}$ mice after an excess iron load. To examine this process with a different experimental paradigm, $Cp^{+/+}$ and $Cp^{-/-}$ mice were made anemic by phlebotomy, removing 15% of their circulating total blood volume daily. Under these circumstances, the delivery of iron from reticuloendothelial stores to the bone marrow becomes an essential and rate-limiting process as the demand for erythropoietic iron increases (24). Over the course of these experiments, mice from both groups became increasingly anemic, such that by day 7 the hemoglobin concentration was 8–10 g/dl (data not shown). Analysis of serum iron concentrations in $Cp^{+/+}$ mice under these circumstances revealed an ability to maintain and eventually elevate serum iron as these mice effectively mobilized iron from reticuloendothelial stores (Fig. 3*C*). In contrast, $Cp^{-/-}$ mice were unable to increase the amount of iron released from reticuloendothelial stores to meet the demand placed by the anemia as evidenced by the fall in serum iron concentration with continued phlebotomy (Fig. 3*C*). These differences in iron mobilization after experimentally induced anemia were apparent when comparing the plasma iron turnover at day 7. While $Cp^{+/+}$ mice were able to increase plasma iron turnover in the face of increased erythropoietic demands, this value was unchanged from baseline in $Cp^{-/-}$ mice, presumably reflecting the differences in serum iron in these animals (Table 2). The ability to maintain serum iron levels in $Cp^{+/+}$ mice under these conditions was dependent upon ceruloplasmin, as the administration of this protein to $Cp^{-/-}$ mice on day 7 led to a prompt increase in serum iron content equivalent to that observed in $Cp^{+/+}$ mice (Fig. 3*C*). In contrast, no change in serum iron content was observed in $Cp^{-/-}$ mice after the injection of apoceruloplasmin (Fig. 3*C*). As observed in the experiments with heat-

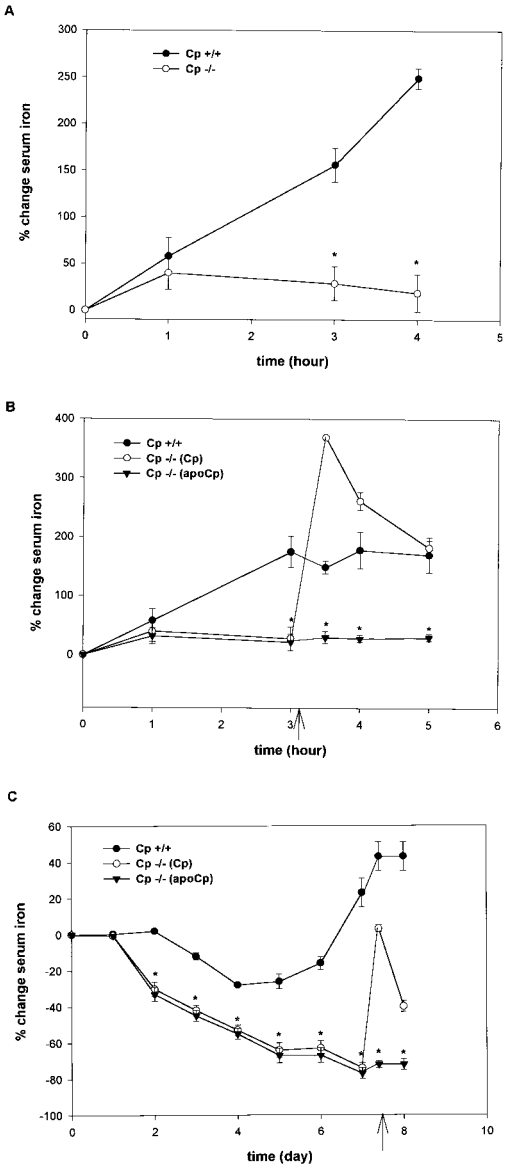

FIG. 3. (*A*) Change in serum iron concentration after the i.v. infusion of damaged red blood cells in 10-wk-old $Cp^{+/+}$ and $Cp^{-/-}$ mice. Results are expressed as means ± standard deviations, $n = 8$ per time point (*, $P < 0.001$). (*B*) Change in serum iron concentration after i.v. infusion of damaged red blood cells. Arrow indicates time of infusion of ceruloplasmin (Cp) or apoceruloplasmin (apoCp) as 6 μg/100 μl of circulating blood volume. Results expressed as means ± standard deviations, $n = 8$ per time point (*, $P < 0.001$). (*C*) Change in serum iron concentration after serial phlebotomy in 10-wk-old $Cp^{+/+}$ and $Cp^{-/-}$ mice. Results are expressed as means ± standard deviations, $n = 6$ per time point (*, $P < 0.001$). Arrow indicates timing of infusion of ceruloplasmin (Cp) or apoceruloplasmin (apoCp) as 6 μg/100 μl of circulating blood volume.

damaged red blood cells, no effect on serum iron was found in phlebotomized $Cp^{+/+}$ mice after ceruloplasmin treatment (data not shown).

Hepatocyte Iron Efflux. The experiments detailed above indicated a role for ceruloplasmin in reticuloendothelial cell iron efflux. However, histological analysis of the liver in $Cp^{-/-}$ mice also revealed clear evidence of excess hepatocyte iron. To determine the mechanisms of hepatocyte iron excess in these animals, we examined iron kinetics after the saturation of the plasma transferrin with iron. Under these circumstances, any iron administered is rapidly taken up by hepatocytes in the liver by non-transferrin-dependent mechanisms (22). This effect of transferrin saturation can be seen in Fig. 4*A,* which demonstrates the marked differences in hepatic iron uptake after ^{59}Fe administration to control and transferrin-saturated mice. Importantly, when ^{59}Fe was administered to $Cp^{+/+}$ and $Cp^{-/-}$ mice after the saturation of plasma transferrin, similar amounts of radioactive iron were detected in the livers of these animals 24 hr after injection (Fig. 4*A*). Detailed kinetic studies revealed no differences in non-transferrin-dependent iron uptake between $Cp^{+/+}$ and $Cp^{-/-}$ mice from 6 to 72 hr after injection (data not shown). This observation indicated that *in vivo* ceruloplasmin plays no role in non-transferrin-dependent iron uptake by hepatocytes. However, when $Cp^{+/+}$ and $Cp^{-/-}$ mice from this same experimental group were subsequently phlebotomized to stimulate the mobilization of hepatic iron stores and then examined 96 hr later, a marked impairment in the efflux of ^{59}Fe from hepatocytes was observed in $Cp^{-/-}$ mice compared with $Cp^{+/+}$ controls (Fig. 4*B*). As was observed in earlier experiments with reticuloendothelial cell iron efflux,

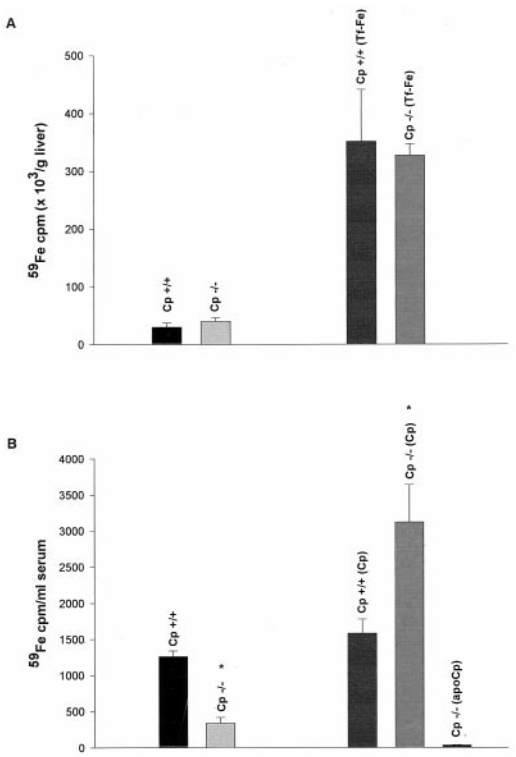

FIG. 4. (*A*) ^{59}Fe uptake in the livers of control and transferrin-saturated (Tf-Fe) 16-wk-old $Cp^{+/+}$ and $Cp^{-/-}$ mice. Results are expressed as means ± standard deviations, $n = 6$ per group. (*B*) Analysis of serum ^{59}Fe in transferrin saturated $Cp^{+/+}$ and $Cp^{-/-}$ mice revealed a statistically significant difference 96 hr after ^{59}Fe injection (*, $P < 0.001$). Results are expressed as means ± standard deviations, $n = 4$ per group. Subsequent infusion of ceruloplasmin (Cp) or apoceruloplasmin (apoCp) as 6 μg/100 μl of circulating blood volume in these mice reveals a statistically significant increase in ^{59}Fe in the serum of $Cp^{-/-}$ mice (*, $P < 0.001$).

the hepatocyte iron efflux observed in $Cp^{+/+}$ mice was dependent upon ceruloplasmin, as administration of this protein to $Cp^{-/-}$ mice resulted in a rapid rise in ^{59}Fe in the serum of these animals (Fig. 4*B*).

DISCUSSION

The data in this manuscript demonstrate the successful creation of a murine model of aceruloplasminemia. When a gene targeting strategy based on a patient splicing mutation that eliminates a homologous region in the human gene and presumably results in protein instability (9, 25) was used, $Cp^{-/-}$ mice were created with no serum ceruloplasmin, progressive accumulation of parenchymal iron, and elevated serum ferritin. Examination of the liver and spleen in $Cp^{-/-}$ mice revealed normal cellular architecture with abundant iron in reticuloendothelial cells and hepatocytes identical to the histology of these organs in affected patients (6–8). At 1 year of age, the oldest animals studied to date, there is no evidence of anemia, diabetes, or neurologic symptoms despite iron accumulation at the corresponding tissue sites (data not shown), suggesting that at this age $Cp^{-/-}$ mice are most similar to patients in the fourth decade of life, in whom significant iron accumulation still precedes by many years the onset of clinical symptoms (5, 26). The absence of iron-deficiency anemia in mice at 1 year of age may reflect alternative sources of ferroxidase activity that may permit release of some iron stores from the reticuloendothelial system.

Ferrokinetic studies in $Cp^{-/-}$ mice revealed no differences in the rate of iron absorption, initial tissue iron distribution, or plasma iron turnover compared with control littermates. As no physiologic mechanism exists to regulate iron excretion, these data suggested that the excessive iron accumulation in these animals results from an imbalance in iron compartmentalization within the red cell cycle (2). To directly test this hypothesis, studies were performed under experimental conditions designed to make the role of ceruloplasmin rate-limiting. Taken together, our results from two different experimental approaches clearly demonstrate a role for ceruloplasmin in determining the rate of iron efflux from the reticuloendothelial system (Figs. 3 and 4). As the hemoglobin concentration remained normal in $Cp^{-/-}$ mice, it remains possible that the excess iron in these animals may also result from an overall decrease in iron excretion not detected in the analysis shown here.

While recent studies *in vitro* have suggested that ceruloplasmin may function to facilitate non-transferrin-dependent cellular iron influx (15, 16), no differences were observed in iron uptake in $Cp^{+/+}$ and $Cp^{-/-}$ mice (Table 2), even under experimental conditions designed to favor this uptake pathway when examined over a 72-hr time frame (Fig. 4*A*). However, these same experiments did reveal a marked impairment in hepatocyte iron efflux in $Cp^{-/-}$ mice (Fig. 4*B*). Thus, as was observed in reticuloendothelial cells, ceruloplasmin plays an essential role in the movement of storage iron out of hepatocytes. As hepatic iron stores are a component of the exchangeable pool of iron within the red cell cycle, these data provide a rational explanation for the hepatic iron accumulation observed in affected patients. These findings are also consistent with the recent observation that serial phlebotomy of a patient with aceruloplasminemia did not result in mobilization of hepatic iron stores (N. Hellman, M. Schaefer, S. Gehrke, P. Stegen, W. Hofmann, J.D.G., and W. Stremmel, unpublished data).

How does ceruloplasmin determine the rate of iron efflux from mobilizable stores in reticuloendothelial cells and hepatocytes? Frieden and colleagues (13) proposed that ceruloplasmin functions as a plasma ferroxidase, providing a gradient for the cellular efflux of Fe^{2+}. This model is supported by data in this paper, which reveal that, under all three experimental

paradigms, the administration of ceruloplasmin to $Cp^{-/-}$ mice resulted in a prompt increase in the serum iron (Figs. 3*B* and 4). A similar ferroxidase mechanism has also been proposed for the function of FET3 in iron uptake in yeast (28, 29) and hephaestin in murine iron absorption (11). These two multicopper oxidases are membrane proteins, and recent studies have revealed a glycosyl-phosphatidylinositol-linked form of ceruloplasmin (30, 31); however, additional experiments are needed to determine whether ceruloplasmin functions in solution or bound to the plasma membrane. The normal iron absorption in $Cp^{-/-}$ mice suggests that hephaestin is required for this process, consistent with the earlier observation of impaired iron transfer in copper-deficient animals. The lack of effect of ceruloplasmin on serum iron in $Cp^{+/+}$ mice and the normal iron kinetics observed in $Cp^{+/-}$ mice (data not shown) indicate that under normal circumstances ceruloplasmin, although essential, is not the rate-limiting factor in iron efflux. The mechanism by which Fe^{2+} crosses the cell membrane also remains unknown. Although recent studies have identified several molecules mediating Fe^{2+} uptake, the role of these proteins in iron efflux has not been explored (32–35).

Whereas most disorders of iron overload reflect changes in the absolute amount of iron, the data in this study reveal that aceruloplasminemia results from iron imbalance caused by impairment in the rate of iron efflux from storage sites. Although the rate of iron efflux in the absence of ceruloplasmin is initially sufficient to maintain erythropoiesis, eventually the accumulation of iron in storage compartments results in decreased serum iron, microcytic anemia, tissue damage, and death (5, 26). As the predominant clinical features of aceruloplasminemia result from iron accumulation in the basal ganglia, it is presumed that ceruloplasmin also functions to determine the rate of iron efflux from storage sites within the central nervous system. Given recent studies suggesting that Friedreich's ataxia may result from impaired mitochondrial iron efflux (36, 37) as well as data indicating an essential role for iron in early central nervous system development (38), further examination of iron kinetics in this compartment in $Cp^{-/-}$ mice is clearly warranted. As illustrated in this study as well as recent work from other laboratories (27, 39, 40), the development of murine models of iron metabolism provides the opportunity to elucidate the pathogenesis of human iron disorders and may permit the development of novel therapeutic approaches to iron overload.

We thank Lou Muglia and Dave Wilson for critical review of the manuscript. These studies were supported by National Institutes of Health Grants HL41536 (J.D.G.) and DK02464 (Z.L.H.). J.D.G. is a recipient of the Burroughs Wellcome Scholar Award in Experimental Therapeutics. Z.L.H. is a Scholar of the Child Health Research Center of Excellence at Washington University School of Medicine (HD33688).

1. Ponka, P., Beaumont, C. & Richardson, D. R. (1998) *Semin. Hematol.* **35,** 35–54.
2. Brittenham, G. M. (1994) in *Iron Metabolism in Health and Disease*, eds. Brock, J. H., Halliday, J. W., Pippard, M. J. & Powell, L. W. (Saunders, Philadelphia), pp. 31–62.
3. Andrews, N. C. & Levy, J. E. (1998) *Blood* **92,** 1845–1851.
4. Bacon, B. R. & Schilsky, M. L. (1999) *Adv. Intern. Med.* **44,** 91–116.
5. Gitlin, J. D. (1998) *Pediatr. Res.* **44,** 271–276.
6. Miyajima, H., Nishimura, Y., Mizoguchi, K., Sakamoto, M., Shimizu, T. & Honda, N. (1987) *Neurology* **37,** 761–767.
7. Logan, J. I., Harveyson, K. B., Wisdom, G. B., Hughes, A. E. & Archbold, G. P. R. (1994) *Q. J. Med.* **87,** 663–670.
8. Morita, H., Ikeda, S., Yamamoto, K., Morita, S., Yoshida, K., Nomoto, S., Kato, M. & Yanagisawa, N. (1995) *Ann. Neurol.* **37,** 646–656.
9. Yoshida, K., Furihata, K., Takeda, S., Nakamura, A., Yamamoto, K., Hiyamuta, S., Ikeda, S., Shimizu, N. & Yanagisawa, N. (1995) *Nat. Genet.* **9,** 267–272.
10. Harris, Z. L., Takahashi, Y., Miyajima, H., Serizawa, M., MacGillivray, R. T. A. & Gitlin, J. D. (1995) *Proc. Natl. Acad. Sci. USA* **92,** 2539–2543.
11. Vulpe, C. D., Kuo, Y. M., Murphy, T. L., Cowley, L., Askwith, C., Libina, N., Gitschier, J. & Anderson, G. J. (1999) *Nat. Genet.* **21,** 195–199.
12. Lee, G. R., Nacht, S., Lukens, J. N. & Cartwright, G. E. (1968) *J. Clin. Invest.* **47,** 2058–2069.
13. Osaki, S., Johnson, D. A. & Freiden, E. (1971) *J. Biol. Chem.* **246,** 3018–3023.
14. Roeser, H. P., Lee, G. R., Nacht, S. & Cartwright, G. E. (1970) *J. Clin. Invest.* **49,** 2408–2417.
15. Mukhopadhyay, C. K., Attieh, Z. K. & Fox, P. L (1998) *Science* **279,** 714–717.
16. Attieh, Z. K., Mukhopadhyay, C. K., Seshadri, V., Tripoulas, N. A. & Fox, P. L. (1999) *J. Biol. Chem.* **274,** 1116–1123.
17. Klomp, L. W. J., Farhangrazi, Z. S., Dugan, L. L. & Gitlin, J. D. (1996) *J. Clin. Invest.* **98,** 207–215.
18. Tybulewicz, V. L., Crawford, C. E., Jackson, P. K., Bronson, R. T. & Mulligan, R. C. (1991) *Cell* **65,** 1153–1163.
19. Robertson, E. J. (1991) *Biol. Reprod.* **44,** 238–245.
20. Osaki, S., Johnson, D. A. & Frieden, E. (1966) *J. Biol. Chem.* **241,** 2746–2751.
21. Torrance, J. D. & Bothwell, T. H. (1980) in *Methods in Hematology: Iron*, ed. Cook, J. D. (Churchill Livingstone, New York), pp. 104–109.
22. Craven, C. M., Alexander, J., Eldridge, M., Kushner, J. P., Bernstein, S. & Kaplan, J. (1987) *Proc. Natl. Acad. Sci. USA* **84,** 3457–3461.
23. Fillet, G., Cook, J. D. & Finch, C. A. (1974) *J. Clin. Invest.* **53,** 1527–1533.
24. Fillet, G., Beguin, Y. & Baldelli, L. (1989) *Blood* **74,** 844–851.
25. Zaitseva, I., Zaitsev, V., Cara, G., Mojhkov, K., Bar, B., Lindley, P. F. (1996) *J. Biol. Inorg. Chem.* **1,** 15–23.
26. Harris, Z. L., Klomp, L. W. J. & Gitlin, J. D. (1998) *Am. J. Clin. Nutr.* **67,** 972S–977S.
27. Fleming, R. E., Migas, M. C., Zhou, X., Jiang, J., Britton, R. S., Brunt, E. M., Tomatsu, S., Waheed, A., Bacon, B. R. & Sly, W. S. (1999) *Proc. Natl. Acad. Sci. USA* **96,** 3143–3148.
28. Kaplan, J. & O'Halloran, T. V. (1996) *Science* **271,** 1510–1512.
29. Radisky, D. & Kaplan, J. (1999) *J. Biol. Chem.* **274,** 4481–4484.
30. Patel, B. N. & David, S. (1997) *J. Biol. Chem.* **272,** 20185–20190.
31. Salzer, J. L., Lovejoy, L., Linder, M. C. & Rosen, C. (1998) *J. Neurosci. Res.* **54,** 147–157.
32. Fleming, M. D., Trenor, C. C. 3rd, Su, M. A., Foernzler, D., Beier, D. R., Dietrich, W. F. & Andrews, N. C. (1997) *Nat. Genet.* **16,** 383–386.
33. Gunshin, H., Mackenzie, B., Berger, U. V., Funshin, Y., Romero, M. F., Boron, W. F., Nussberger, S., Gollan, J. L. & Hediger, M. A. (1997) *Nature (London)* **388,** 482–488.
34. Yu, J., Yu, Z. K. & Wesling-Resnick, M. (1998) *J. Biol. Chem.* **273,** 34675–34678.
35. Rouault, T. & Klausner, R. (1997) *Curr. Top. Cell Regul.* **35,** 1–19.
36. Babcock, M., de Silva, D., Oaks, R., Davis-Kaplan, S., Jiralerspong, S., Montermini, L., Pandolfo, M. & Kaplan, J. (1997) *Science* **276,** 1709–1712.
37. Radisky, D. C., Babcock, M. C. & Kaplan, J. (1999) *J. Biol. Chem.* **274,** 4497–4499.
38. Levy, J. E., Jin, O., Fujiwara, Y., Kuo, F. & Andrews, N. C. (1999) *Nat. Genet.* **21,** 396–399.
39. Poss, K. D. & Tonegawa, S. (1997) *Proc. Natl. Acad. Sci. USA* **94,** 10919–10924.
40. Zhou, X. Y., Tomatsu, S., Fleming, R. E., Parkkila, S., Waheed, A., Jiang, J., Fei, Y., Brunt, E. M., Ruddy, D. A., Prass, C. E., *et al.* (1998) *Proc. Natl. Acad. Sci. USA* **95,** 2492–2497.